


ARTICLE

Enhancement of angiogenin inhibition by polyphenol-capped gold nanoparticles

Atashi Panda¹ | Siddhant Karhadkar¹ | Bidisha Acharya² | Anwesha Banerjee¹ | Soumya De² | Swagata Dasgupta¹ 

¹Department of Chemistry, Indian Institute of Technology Kharagpur, Kharagpur, India

²School of Bioscience, Indian Institute of Technology Kharagpur, Kharagpur, India

Correspondence

Swagata Dasgupta, Department of Chemistry, Indian Institute of Technology Kharagpur, Kharagpur-721302, India.
Email: swagata@chem.iitkgp.ac.in

Funding information

Council of Scientific and Industrial Research, India, Grant/Award Number: 01(2959)/18/EMR-II; Indian Institute of Technology Kharagpur

Abstract

Angiogenin (Ang), is a ribonucleolytic protein that is associated with angiogenesis, the formation of blood vessels. The involvement of Ang in vascularisation makes it a potential target for the identification of compounds that have the potential to inhibit the process. The compounds may be assessed for their ability to inhibit the ribonucleolytic activity of the protein and subsequently blood vessel formation, a crucial requirement for tumor formation. We report an inhibition of the ribonucleolytic activity of Ang with the gallate containing green tea polyphenols, ECG and EGCG that exhibits an increased efficacy upon forming polyphenol-capped gold nanoparticles (ECG-AuNPs and EGCG-AuNPs). The extent of inhibition was confirmed using an agarose gel-based assay followed by fluorescence titration studies that indicated a hundred fold stronger binding of polyphenol-capped gold nanoparticles (GTP-AuNPs) compared to the bare polyphenols. Interestingly, we found a change in the mode of inhibition from a noncompetitive type to a competitive mode of inhibition in case of the GTP-AuNPs, which is in agreement with the 'n' values obtained from the fluorescence quenching studies. The effect on angiogenesis has also been assessed by the chorioallantoic membrane (CAM) assay. We find an increase in the inhibition potency of GTP-AuNPs that could find applications in the development of anti-angiogenic compounds.

KEYWORDS

affinity values, CAM assay, cloning, competitive inhibition, *FlexX* molecular docking, fluorescence spectroscopy, green tea polyphenols, human angiogenin, kinetics, noncompetitive inhibition

1 | INTRODUCTION

Human angiogenin (Ang), a kidney-shaped cationic protein with an isoelectric point above 9.0, is a potent blood vessel inducer, a crucial

requirement for tumorigenesis.^[1] Among other angiogenic molecules, Ang is unique in that it is a ribonucleolytic enzyme^[2] with an amino acid sequence that is 33% identical to that of pancreatic ribonuclease A (RNase A).^[3] Ang being an angiogenic factor, plays a major role in the growth and establishment of human tumors, whereas RNase A does not.^[4] Ang exhibits a characteristic ribonucleolytic activity that is several orders of magnitude weaker than that of pancreatic RNase A in standard assays^[5,6] but nonetheless has been reported to be essential for its angiogenic activity.^[7] Angiogenin has thus been projected as a pharmaceutical

Abbreviations: Atomic force microscopy, AFM; Chorioallantoic membrane, CAM; Cyclic cytidine monophosphate, cCMP; Dynamic Light Scattering, DLS; Epicatechin gallate-capped gold nanoparticles, ECG-AuNPs; Epicatechin gallate, ECG; Epigallocatechin gallate-capped gold nanoparticles, EGCG-AuNPs; Epigallocatechin gallate, EGCG; Green tea polyphenol-capped gold nanoparticles, GTP-AuNPs; Green tea polyphenols, GTPs; Human angiogenin, Ang; Sodium dodecyl sulfate-polyacrylamide gel electrophoresis, SDS-PAGE; Tris-Acetic acid-EDTA, TAE.

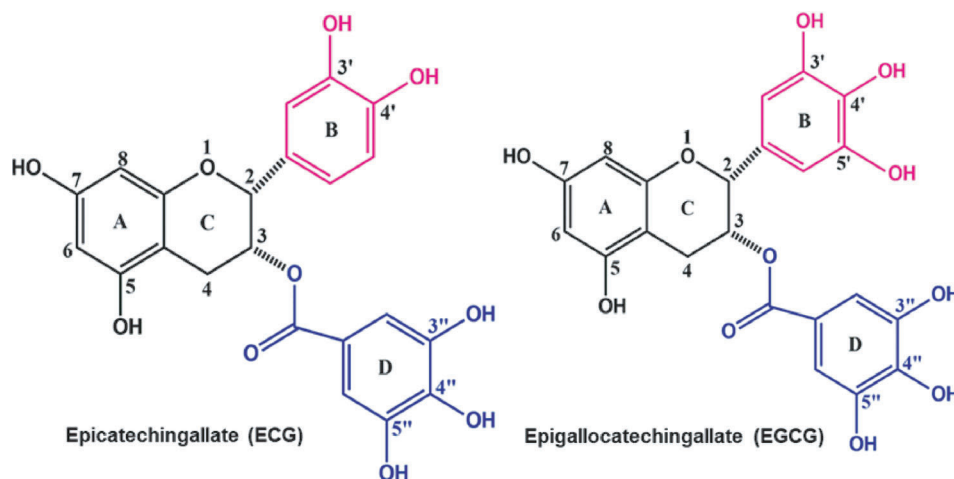


FIGURE 1 Structures of green tea polyphenols containing gallate moiety

target for the development of small-molecule inhibitors of its enzymatic activity that can be developed as novel anti-angiogenic agents.^[8]

An article in *Nature* around two decades ago emphasized that angiogenesis was inhibited by drinking tea.^[9] We had subsequently shown the effects of green tea polyphenols on angiogenin-induced angiogenesis and RNase A.^[10,11] Considering the adverse effects of angiogenin, many studies have been carried out using green tea polyphenols (GTPs) that have focused on the inhibition of the growth of new blood vessels.^[12] The effect of green tea on anti-angiogenesis has been attributed to its antioxidant activities.^[13] Investigations from our laboratory investigated the specific role of the gallate moiety of GTPs in the inhibition of Ribonuclease A (RNase A).^[14] In the present study, we show the effect of GTPs, derivatives of gallic acid, ECG ((-)-Epicatechin gallate) and EGCG ((-)-Epigallocatechin gallate; Figure 1) on the ribonucleolytic activity and their mode of binding to Ang as well as a change in the mode of inhibition when bound to gold nanoparticles.

Despite the enormous potential of the GTPs to act as anti-cancer agents, these polyphenols have low solubility and short half-life, which limits its utility in clinical settings. Polyphenol capping using specific nanocarriers, increases its bioavailability and reduces premature degradation and increases target specificity due to nanoparticle surface functionalisation. In this study, the binding of ECG and EGCG to Ang has been monitored and compared with the efficacy of the inhibition with ECG- and EGCG-capped gold nanoparticles.

The focus is primarily on the ribonucleolytic activity of Ang, which affects its angiogenic activity. The protein has been cloned and expressed using the Ang gene. The ribonucleolytic site of Ang is constituted of multiple subsites,^[15,16] that bind to the phosphate, nucleobase and sugar components of the RNA molecule. The three catalytic residues of RNase A, His 12, Lys 41, and His 119 of the P1 subsite (where cleavage of the phosphodiester bond occurs)^[8] are conserved in Ang as residues His 13, Lys 40, and His 114.^[17]

Inhibition of the ribonucleolytic activity of Ang may be possible by directly blocking the active site that should in turn lead to a disruption of its angiogenic activity.

2 | MATERIALS AND METHODS

2.1 | Materials

The plasmid vector pCMV3-SP-N-His encoding Ang was purchased from Sino Biological Inc. (China) and other chemicals from Sigma Chemical Co. (St. Louis). The concentration of 2',3'-cCMP was determined from the following data: $\epsilon_{268} = 8500 \text{ M}^{-1} \text{ cm}^{-1}$.^[18]

2.2 | Methods

2.2.1 | Cloning and expression of Ang gene

The gene encoding Ang was cloned between the NdeI and BamHI restriction sites of pET28a vector. Protein expression and purification was carried out as mentioned earlier.^[7] Briefly, the protein was expressed as inclusion bodies in *E. coli* BL21 (DE3) cells when induced with 1 mM IPTG at 37 °C. The cells were harvested for 4 h post induction and the cell pellet resuspended in 25 ml lysis buffer (23% sucrose, 500 mM Tris-HCl, 1 mM EDTA, and 100 mM NaCl, pH 8.2) containing lysozyme and incubated for 1 h at 37 °C and lysed by sonication. The pellet, containing inclusion bodies collected by centrifugation was washed thrice with 10 ml of wash buffer A (50 mM Tris, 100 mM NaCl, 1 mM EDTA, 0.5% Triton, pH 8.2), and twice with 10 ml of wash buffer B (50 mM Tris, 100 mM NaCl, 1 mM EDTA, pH 8.2). The resulting pellet was resuspended in 10 ml 7 M Guanidine-HCl, 0.15 M reduced glutathione, 0.1 M Tris-HCl, 2 mM EDTA, pH 8.2.

2.2.2 | Refolding and purification of Ang from inclusion bodies

The solution containing inclusion bodies was added dropwise with gentle stirring to 500 ml of refolding buffer containing 0.5 M L-Arginine-HCl, 0.6 mM oxidized glutathione and left under stirring conditions for 24 h at 4 °C. The volume was 10-fold reduced and the solution dialysed for 48 h in 20 mM Tris-HCl (containing 100 mM NaCl) at pH 7.4. The final volume was then injected into a 4 ml Ni²⁺-NTA affinity column (GE Healthcare) and the purified protein obtained using a gradient of wash buffer (50 mM Tris-HCl and 100 mM NaCl at pH 8.2) and elution buffer (50 mM Tris-HCl, 100 mM NaCl and 500 mM imidazole at pH 8.2). The fractions containing the purified protein were assessed from SDS-PAGE.

2.2.3 | Agarose gel-based assay

The effect of Diethyl pyrocarbonate (DEPC) on the ribonucleolytic activity of Ang was monitored via an agarose gel-based assay. Ang (5 µM, 10 µl) in 20 mM phosphate buffer was incubated with DEPC (10 µM) for 2 h. The solution was then treated with 20 µl RNA (2.5 mg/ml) for 90 min. Then 10 µl sample buffer was added and 20 µl aliquot was used for electrophoresis.

Inhibition of Ang by the ligands was also analyzed qualitatively by monitoring the degradation of RNA in an agarose gel-based assay.^[19] In this method Ang (5 µM, 5 µl) was mixed with polyphenols (10 µl; 0–200 µM) in 20 mM phosphate buffer (pH 7.4) and incubated at 37 °C for 30 min. To the incubated mixture, 10 µl RNA (5 mg/ml) was added and kept for 2.5 h. The reaction mixture was mixed with 5 µl sample buffer and from the total solution 20 µl aliquot was loaded onto 1.1% agarose gel and the gel was run in 0.04 M TAE buffer (pH 8.0). After electrophoresis the undegraded tRNA was visualized under UV light after staining with ethidium bromide.

2.2.4 | Docking studies

To assess the site of binding of ECG and EGCG with Ang, docking studies were performed. The crystal structure of Ang (PDB entry for human angiogenin: 1B1I^[20]) was obtained from the Protein Data Bank^[21] and used for the study. The structures of all the ligands were drawn in Sybyl 6.92 (Tripos Inc., St. Louis) and their energy-minimized conformations were obtained with the help of the Tripos force field using MMFF94 charges with a gradient of 0.005 kcal/mol with 1000 iterations using all other default parameters. The FlexX program that is part of the Sybyl suite was used to perform the docking studies and their poses visualized with the help of PyMol.^[22] The conformation with the lowest score was then selected for measuring the polar contacts between the ligands and the protein. The affinity values for ECG and EGCG were determined from AutoDock Vina with the center positioned at the following coordinates: $x = 11.275$, $y = 10.855$, and $z = 11.709$ and grid size $102 \text{ Å} \times 118 \text{ Å} \times 126 \text{ Å}$.^[23]

2.2.5 | Accessible surface area calculation

The accessible surface area (ASA) of angiogenin and their docked complexes with ECG and EGCG were calculated using the NACCESS^[24] program. The structures corresponding to the lowest affinity value (as obtained from AutoDock Vina) were used for ASA study. The following expression has been used to measure the change in ASA for i 'th residue.

$$\Delta ASA^i = ASA^i_{Ang} - ASA^i_{Ang-ECG/EGCG}$$

If the residue lost more than 10 Å^2 when going from free to complex state it was considered as being involved in the interaction.^[14]

2.2.6 | Enzyme kinetics

The rate of inhibition of protein by ligands was measured by a spectrophotometric method, described by Anderson *et al.*^[18] using 2',3'-cCMP as the substrate, in oligo vinyl sulfonic acid free 0.1 M Mes-NaOH buffer (pH 6.0) containing 0.1 M NaCl.^[25] The concentration of the substrate was varied from 0.32 to 1.12 mM, and the varying inhibitor concentration, with 0.01 mM Ang. The inhibition constant values and the nature of the curve has been determined using a modified Lineweaver Burk (LB) plot. It may be noted that there is no interaction between the substrate and the ligands.

2.2.7 | Fluorescence spectroscopy

The interaction of polyphenols with Ang were estimated from an intrinsic fluorescence quenching mechanism due to the presence of the sole Trp in Ang using Horiba Jobin Yvon-Spex Fluorolog-3 spectrofluorimeter. The titration was carried out in 20 mM phosphate buffer (pH 7.0), keeping the concentration of Ang at 5 µM. The samples were excited at 295 nm and the emission range set from 310 to 450 nm. Both the excitation and emission slits were 5 nm with an integration time of 0.3 s.

2.2.8 | Chorioallantoic membrane assay

The *in vivo* effect of purified Ang and small molecules were assessed by a Chorioallantoic membrane (CAM) assay.^[26] Fertilized hen eggs of White Leghorns were acquired on embryonic day 0 from a local poultry farm. The eggs were incubated vertically at 37 °C, in 60%–65% humidified atmosphere. On day 3, a tiny window was made by removing the shell under aseptic conditions. The window was resealed with parafilm and kept inside an incubator until day 7. Sample solutions (10 µl, 5 µM Ang with 0.1% GTPs and GTP-AuNPs) were prepared in saline buffer (pH 7.4) and were each added over a transparent plastic disc and dried in a laminar flow hood. On day 7, the discs were placed on top of the CAM in an inverted position and returned to the incubator for 72 h (until day 10). CAM

transformation was assessed by visual inspection and photographed with a digital camera (Nikon P530). The variation in the number of blood vessels for the control and samples were measured by Kodak MI software.

2.2.9 | Preparation of polyphenol-capped gold nanoparticles (GTP-AuNPs)

Available in the Supplementary information.

2.2.10 | Statistical analysis

Each experiment was performed at least three times and the data represented as mean \pm SD. For the *in-vivo* study, the CAM assay was performed with a total of 20 eggs. The relative blood intensity has been determined for five eggs in each sample set. Comparisons between the groups were done by performing a one-way ANOVA followed by Bonferroni post-*t*-test with *P* value <0.01, indicating statistical significance.

3 | RESULTS AND DISCUSSION

The over-expression and purification of native Ang has been accomplished and *in vitro* and *in vivo* assays were developed to monitor the effect of binding of the polyphenols and the polyphenol-capped gold nanoparticles to the protein.

3.1 | Cloning, expression, and purification of Ang

Wild type Ang protein contains 123 amino acid giving a molecular weight of 14 kDa but the Ang protein used for this study contains 6His-tag at the N-terminal, which increases its amino acid residues to

144 and changes its molecular weight to 16 kDa. No significant change in the overall *pI* of the protein was observed. Due to the small size of the His tag it is believed that they do not significantly interfere with the structure and function of the protein, therefore, the experiments were performed with His tagged protein and the protein purification protocol has been optimized accordingly.

Ang was expressed as inclusion bodies in *E. coli* BL21(DE3) cells (Figure 2A) and obtained in functional form after *in vitro* refolding followed by purification in an Ni-NTA affinity column. The purity of the eluted protein was assessed by 15% SDS-PAGE. The Ang protein appeared as a prominent band on SDS-PAGE at 16 kDa, in the monomeric form (Figure 2B).

3.2 | Characterization and inhibition assessed by an agarose gel-based assay

Ang follows the same catalytic mechanism as RNase A with the His residues involved in the mechanism that cleaves RNA.^[27] Upon treatment with DEPC (diethyl pyrocarbonate), a His-DEPC adduct is formed rendering the protein unable to cleave RNA as a result of which the ribonucleolytic activity of Ang is abolished. Characterization by an agarose gel-based assay using DEPC confirmed that the purified protein is in its native state and contains His at its active site. The ribonucleolytic activity of Ang due to His residues present at the active site decreases (Figure 3) as can be observed from the band intensity of lane 2 (containing Ang + RNA) compared to that of the control (lane 1; containing only RNA). As mentioned earlier, the decrease in the intensity is not very significant compared to RNase A,^[20] because the ribonucleolytic activity of Ang is several orders of magnitude weaker.^[5,6] Lane 1 and lane 3 being of nearly the same intensity, suggests that DEPC modified Ang is unable to cleave RNA, because of the formation of the His-DEPC adduct confirming the presence of His residues at the active site of the isolated Ang.

Following the procedure mentioned in Section 2.2.3, an agarose gel-based assay was performed for Ang with ECG and ECGG to

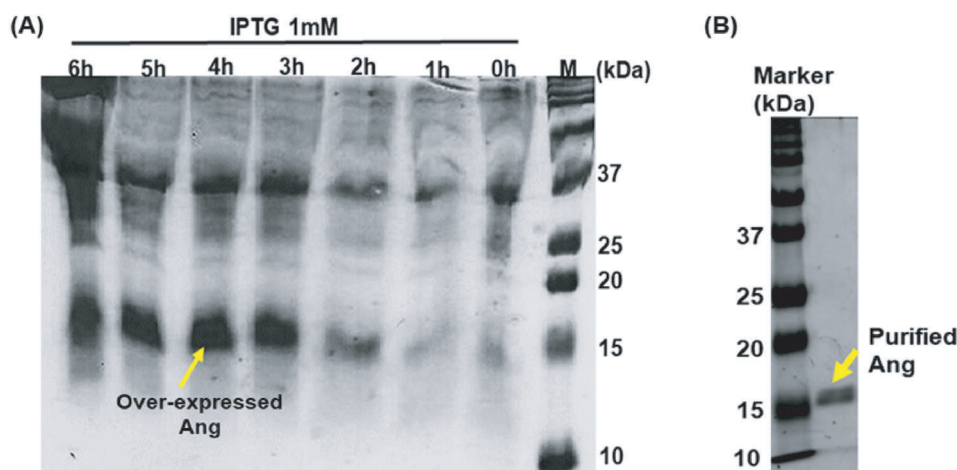


FIGURE 2 15% SDS-PAGE shows A, an increase in expressed protein concentration with time. B, Purified monomeric protein collected from Ni-NTA column chromatography

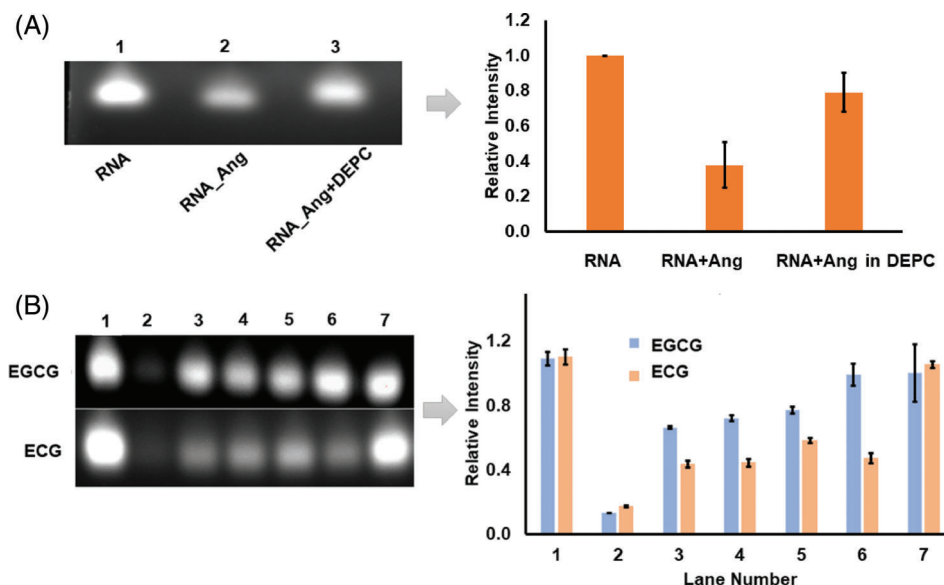


FIGURE 3 A, Agarose gel image confirming the refolding of protein in its native state along with Histogram Plot showing the presence of Histidine residue at the active site. B, Agarose gel image for inhibition of Ang by GTPs: Lane1: tRNA, Lane2: tRNA + Ang, Lane3: tRNA + Ang + ECG/EGCG (25 μ M), Lane 4: 7 contains ECG/EGCG 50, 75, 100, and 200 μ M, respectively, along with the histogram showing the increase in intensity of RNA with increase in concentration of inhibitors ($P < 0.01$, experiments are performed thrice and mean value is taken for plotting the histograms)

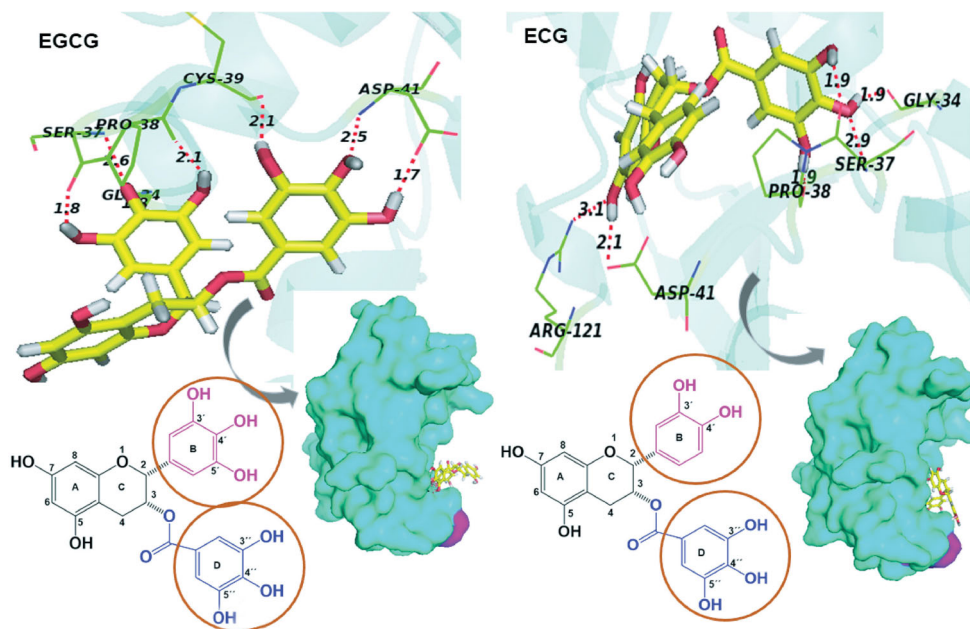


FIGURE 4 Docked conformations of the GTPs with Human Angiogenin (1B1I). Hydrogen bonds are shown as dashed lines. Line structure shown in green color represents the amino acid residues interacting with the ligands. Below at right side of every docked presentation, the surface diagram of the protein is presented and left side shows the binding moieties of the GTPs

study their inhibitory efficacy against the ribonucleolytic activity of Ang (Figure 3B). The intense band in Lane 1 corresponds to RNA and the faint intensity of the band in lane 2 is due to the degradation of RNA by Ang alone. Lanes 3–7 correspond to RNA with Ang in presence of increasing concentrations of ECG/EGCG (25–200 μ M).

The gradual increase in intensity of bands from lanes 3 to 7 for both EGCG and ECG indicates inhibition of the ribonucleolytic activity. For EGCG, it is observed that a relatively lower concentration is required for inhibition of the enzymatic activity compared to ECG which is apparent from the increase in the intensity. This makes

TABLE 1 Distance (Å) between amino acid residues of Ang (1B1I) and the GTPs

Ang (1B1I)	ECG	EGCG
Gly 34 O	1.9 (4''-H Ring D)	1.8 (4'-H Ring B)
Ser 37 O _γ	1.9 (3''-H Ring D)	1.8 (3'-H Ring B)
Ser 37 N	2.9 (4''-O Ring D)	2.6 (4'-O Ring B)
Pro 38 O	1.9 (5''-H Ring D)	2.1 (5'-O Ring B)
Cys 39 O	–	2.1 (3''-H Ring D)
Asp 41 O _γ	2.1 (7-H Ring A)	1.7 (5''-H Ring D)
Asp 41 N	–	2.5 (4''-O Ring D)
Arg 121 N _η 1	3.1 (7-O Ring A)	–

EGCG a comparatively better inhibitor with respect to ECG. The histogram shows statistically significant data ($P < 0.01$) with relatively higher band intensity for EGCG compared to ECG, confirming that among the two GTPs, EGCG is more potent inhibitor of the ribonucleolytic activity of Ang.

3.3 | Docking and ASA studies to identify interacting amino acid residues

The inhibition of several proteins using bioflavonoids present in green tea and black tea has previously been reported.^[28,29] The docking characteristics of Ang after binding with the polyphenols ECG and EGCG resemble the RNase A docked pose with the same ligand (in an earlier study from this laboratory).^[14]

The docked poses shown in Figure 4, reveal that random coils and turns are mostly involved in binding with the polyphenol involving amino acid residues Gly 34, Ser 37, Pro 38, Cys 39, and Asp 41 within a distance of 4 Å. All the possible interactions of ECG and EGCG involve rings B and D with very few interactions observed with rings A and C as ring A protrudes outwards and interactions are preferred with the gallate moiety (Ring D).

Angiogenin has three important sites: (a) the ribonucleolytic site comprised of His 13, Lys 40 and His 114 as mentioned earlier; (b) a nuclear translocation site spanning residues ₃₁RRRGL₃₅; and (c) a cell-binding site from residues 60 to 68. Both ECG and EGCG are involved in interactions with residues in the region from 34 to 41 that includes Lys 40, a member of the ribonucleolytic site which is responsible for the hydrolysis of RNA.^[30,31] This inclusion also accounts for the inhibition of catalytic activity. A list of all the interacting amino acids and the corresponding bond distances formed with the ligands are given in Table 1. The affinity values obtained from the docking studies performed in *AutoDock Vina* shows that EGCG exhibits a higher affinity (~ -6.1 kcal/mol) compared to ECG (~ -5.2 kcal/mol) towards the protein which is in good agreement with the agarose gel-based assay that also indicated that EGCG exhibits better anti-ribonucleolytic behavior in Ang compared to ECG.

Apart from the ribonucleolytic site, the nuclear translocation site is essential for its angiogenic activity. This generates a nuclear

TABLE 2 Change in accessible surface area (Δ ASA) in Å² of interacting residues of Ang (free), and its complexes with ECG and EGCG

Residues	Δ ASA–ECG	Δ ASA–EGCG
His-8	3.90	0.00
Gln-12	17.18	6.87
His-13	7.95	0
Gln-34	12.18	14.36
Leu-35	11.92	13.37
Ser-37	23.65	25.11
Pro-38	35.59	45.81
Cys-39	9.21	7.43
Lys-40	57.96	47.24
Asp-41	31.56	22.85
His-114	16.06	0.00
Leu-115	2.44	0.00
Arg-121	0.00	1.57

localisation signal (NLS) which is responsible for the transportation of angiogenin to the nucleus followed by uptake through endothelial cells.^[30] Docking studies reveal an involvement of residues 34–41 that partially overlaps with the nuclear localisation signal^[32,33] ₃₁RRRGL₃₅.

Interaction with Gly 34 (a member of the nuclear translocation site) implies that this is expected to inhibit the angiogenic property of the protein as well, which is later confirmed by an *in vivo* study. The interaction of ECG and EGCG with Ang is similar to that of RNase A which had been reported earlier from this laboratory where an indirect effect on the active site residues was observed.^[14] On similar lines the active site His residues, His 13 and His 114 do not show any substantial change in their accessible surface area. The other residue that is part of the catalytic triad is Lys 40 that is involved in an H bond to the pentavalent transition state. Significant changes in the ASA of Lys 40 have been observed for both ligands which implies that the ligands interact directly with Lys 40 thus making it less accessible to the solvent, as a result of which the catalytic activity of Ang is inhibited. Additionally, interactions with His 8 and Arg 5 that are part of the cation cluster of the P₂ binding subsites of Ang are observed, similar to Lys 7 and Arg 10 that participate indirectly in RNA hydrolysis.^[34] The docking poses of GTPs, corroborate the noncompetitive nature of binding also observed in the kinetic studies.

The importance of gallate moiety has been observed in several proteins including RNase A where the inhibitory effect was higher for ECG and EGCG. Results from the docking studies indicate the involvement of ring D, the gallate moiety in interactions with the amino acid residues of the protein. The agarose gel-based study shows qualitatively that the polyphenols are able to inhibit the ribonucleolytic activity, but without directly affecting its ribonucleolytic site (as observed from docking poses and corresponding ASA values). This points towards an allosteric mode of inhibition that occurs for Ang when bound to gallate containing green tea polyphenols. This observation is similar to that of RNase A where a noncompetitive mode of binding

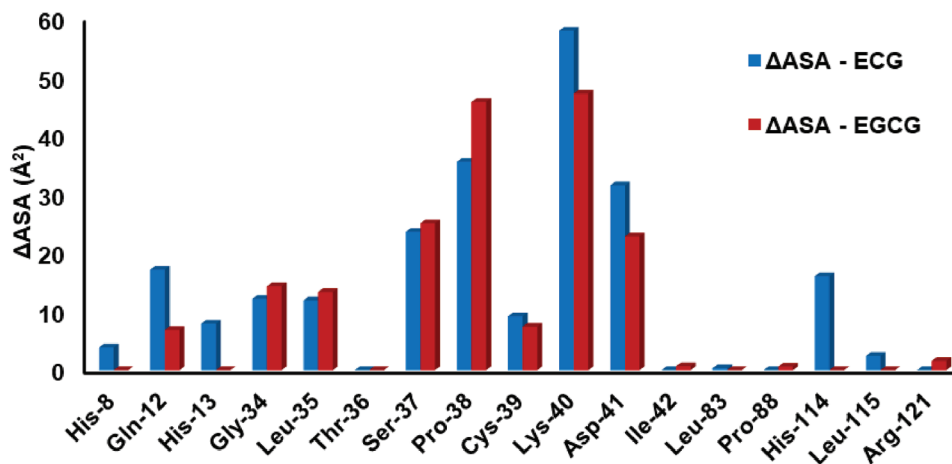


FIGURE 5 Change in ΔASA (\AA^2) of residues involved in the docking of ECG and EGCG to Ang

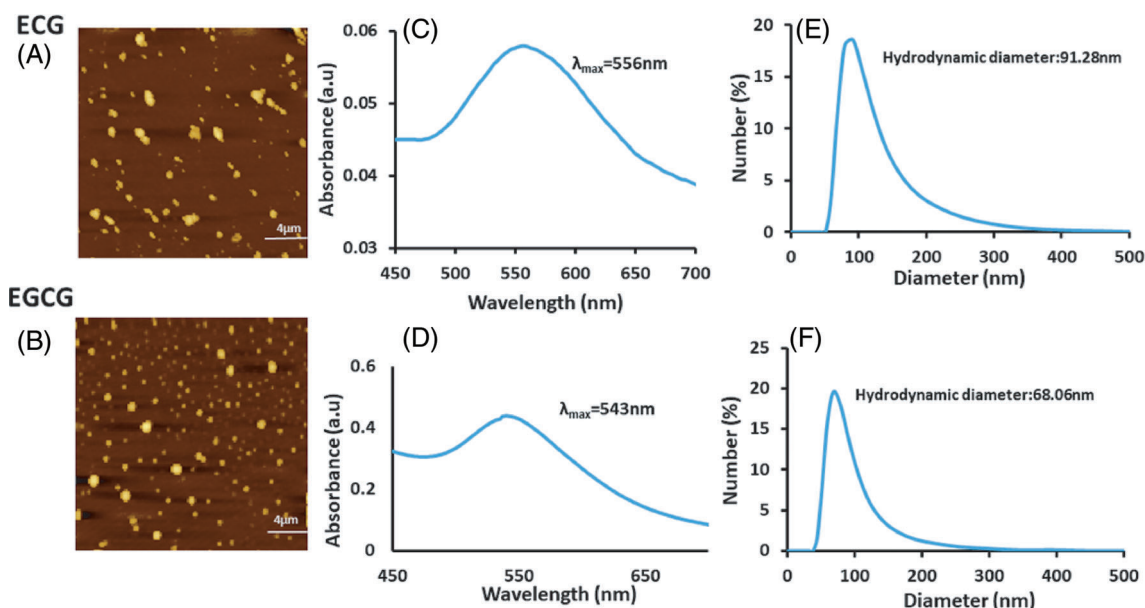


FIGURE 6 A,B, Characterization of ECG-AuNPs and EGCG-AuNPs. AFM images of the nanoparticles shows particle are spherical in shape with a diameter of ~ 82.5 and ~ 54.6 nm, respectively. C,D, UV-Vis spectra shows absorption maxima of 556 and 543 nm of the ECG and EGCG gold nanoparticles, respectively, and E,F, The DLS measurement showing their hydrodynamic diameter

was observed for these ligands.^[14] This preliminary study gives us a possible reason to study the effect of polyphenol-capped gold nanoparticles.

To further identify the residues taking part in the interaction, we calculated the change in accessible surface areas (ΔASA) of the residues of Ang and Ang-polyphenol complex as shown in Table 2. The loss in accessible surface area due to the docking of ECG is $\sim 72 \text{ \AA}^2$ which is about half of that of EGCG ($\sim 148 \text{ \AA}^2$), implying that the latter covers a larger surface area on the protein molecule despite the similarity in the structure. We observe that the charged residues near the binding site lose considerable amount of ASA in the process (Figure 5). In addition Ser-37, Pro-38, Lys 40, and Asp-41, suffers a substantial change in ASA due to electrostatic

interactions and H-bond interactions, when complexed with both ECG and EGCG.

3.4 | Spectroscopic and microscopic characterization of the prepared GTP-AuNPs

Following the synthesis of the GTP-AuNPs (provided in the Supplementary information), the nanoparticles were characterized by AFM, UV-Vis spectroscopy and DLS (Figure 6). Morphological features were analyzed using AFM techniques where it shows that the nanoparticles are spherical in shape and uniformly distributed over the surface with a diameter of ~ 82.5 nm for ECG-AuNPs and ~ 54.6 nm for EGCG-

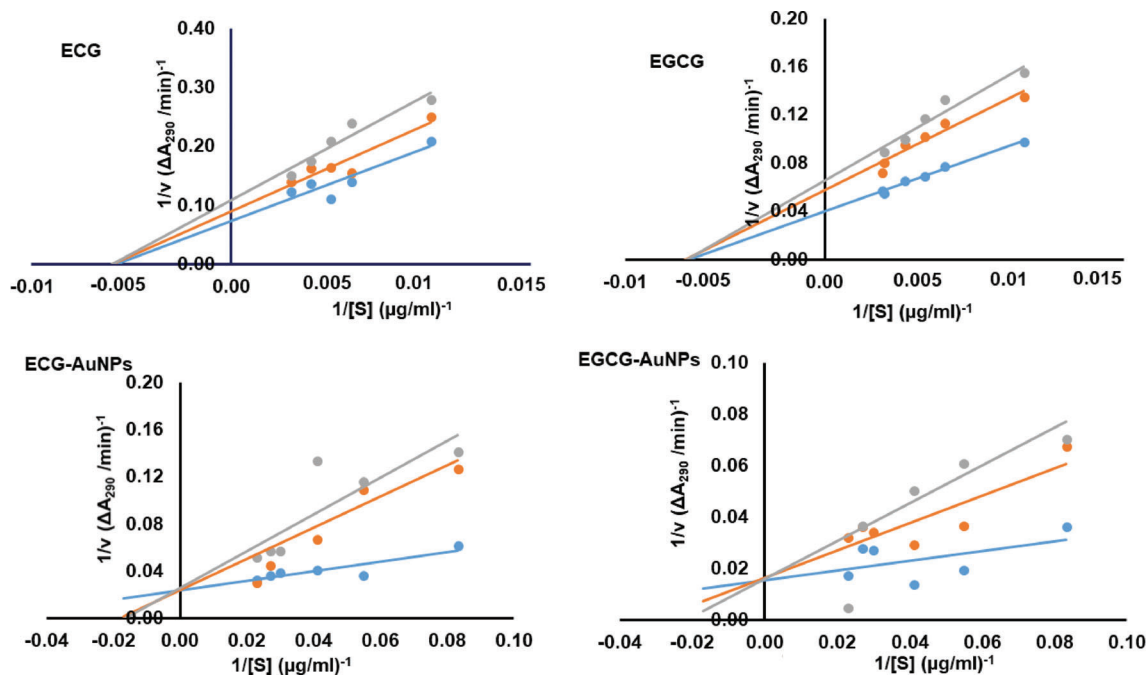


FIGURE 7 Lineweaver-Burk plots for the mentioned compounds, where the symbol $l = 0 \mu\text{g/ml}$ (Blue), $l = 4 \mu\text{g/ml}$ (Orange), and $l = 8 \mu\text{g/ml}$ (Gray dot), with varying concentrations of the substrate 2',3'-cCMP (S)

TABLE 3 Comparison of efficiency of inhibitors for GTPs and GTP-AuNPs as obtained from kinetic experiments

Inhibitors	Type of inhibition	Inhibition constant K_i
ECG	Noncompetitive	18.35 ± 2.1
EGCG	Noncompetitive	13.27 ± 0.8
ECG-AuNPs	Competitive	4.12 ± 0.5
EGCG-AuNPs	Competitive	3.61 ± 2.3

AuNPs. UV-Vis spectra shows a λ_{max} at 556 nm for ECG-AuNPs and EGCG-AuNPs shows a λ_{max} of 543 nm.

The occurrence of a red shift of AuNPs has been attributed to an increase in particle size.^[35] DLS experiments were carried out to determine the size of the nanoparticles for both the polyphenols. It was observed that the average hydrodynamic size of ECG-AuNPs is 91.28 ± 8 nm and that of EGCG-AuNPs is 68.06 ± 10 nm. Quantitative information about the physicochemical properties of ECG and EGCG was obtained from Open Babel descriptor.^[36] The values (177.14 \AA^2 for ECG and 197.37 \AA^2 for EGCG) of the topological polar surface area of ECG indicate that it is less soluble in aqueous medium compared to EGCG. A substantial increase in the diameter of ECG-AuNPs as observed in both the DLS and AFM studies is likely due to the formation of agglomerates, because of the low solubility of ECG in aqueous medium compared to EGCG. The formation of stable GTP-AuNPs was confirmed after storing the sample at 4°C for 4 months, as no precipitation was observed and AFM images (Figure S1) show well dispersed spherical nanoparticles over the surface. As gold nanoparticle stabilization

and formation cannot take place without any capping/stabilizing agent, this confirms that GTPs were involved in stabilizing the AuNPs by forming a layer around its surface. The zeta potential values indicate that the GTP-AuNPs are negatively charged with zeta potential values for ECG- and EGCG-AuNPs of -1.3 ± 0.6 mV and -1.7 ± 0.3 mV, respectively.

3.5 | *In vitro* and *in vivo* study of polyphenol-capped gold nanoparticles

Earlier reports on the release of polyphenol-capped gold nanoparticles have demonstrated a sustained release under both *in vitro* and *in vivo* conditions.^[37–39] Based on this observation, we have carried out some experimental techniques to study the interaction between the protein and the polyphenols. To determine the mode of inhibition of the compounds against Ang and the inhibition constants of the protein, kinetic experiments were performed. The Lineweaver-Burk plots for ECG, EGCG, ECG-AuNPs, and EGCG-AuNPs are shown in Figure 7, and the mode of inhibition and the inhibition constant values are presented in Table 3.

It was found that all the polyphenols bind in a noncompetitive fashion despite of the involvement of the active site residues as observed from the ASA study, which indicates that the inhibitors bind to a site other than the ribonucleolytic site but nevertheless disrupts the ribonucleolytic activity.

Binding to the active site provides evidence of the presence of competition between the inhibitors and the substrate, while the preference for the allosteric site of the ligand indicates a lack of competition. Nevertheless, exceptions for this notion do exist.^[40] For the

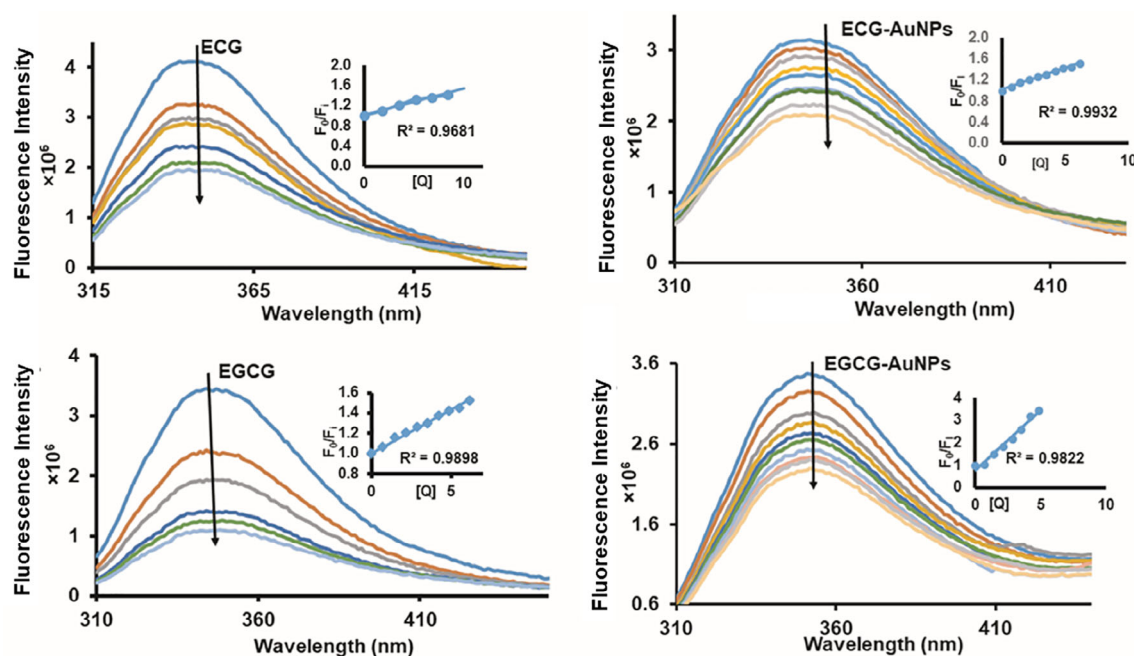


FIGURE 8 Fluorescence emission spectra ($\lambda_{\text{ex}} = 350$ nm) of Ang ($5 \mu\text{M}$) in absence (top line) and presence of different polyphenols in 20 mM Phosphate buffer pH 7.0 at 25°C . Stern-Volmer plots for the interaction of different polyphenols with Ang (Inset)

TABLE 4 Binding parameters of Ang with GTPs and GTP-AuNPs as obtained from fluorescence titration experiment

Inhibitors	Number of binding sites (n)	Binding constant (K_b)	Stern-Volmer constant (K_{sv}) in Lg^{-1}
ECG	0.8304 ± 0.01	$0.62 \pm 0.02 \times 10^2$	$0.51 \pm 0.06 \times 10^2$
EGCG	0.894 ± 0.03	$0.78 \pm 0.07 \times 10^2$	$0.86 \pm 0.02 \times 10^2$
ECG-AuNPs	1.03 ± 0.12	$8.61 \pm 0.72 \times 10^4$	$0.08 \pm 1.35 \times 10^4$
EGCG-AuNPs	1.83 ± 0.03	$16.82 \pm 0.93 \times 10^4$	$0.47 \pm 0.91 \times 10^4$

polyphenols, we observe a noncompetitive inhibition pattern of inhibition indicating an indirect effect on the ribonucleolytic site (His 13, Lys 40, His 114). However, the ΔASA differences indicated in Table 2 for ECG show that there is a loss of surface area for the active site residues. The docking poses show that the ECG molecule is at an allosteric site but within 6 \AA of the active site His residues. Due to this proximity the substrate binding is likely to be affected despite the ligand not directly going to the ribonucleolytic site. On the other hand, EGCG shows no ΔASA change for the active site His residues as they are at a distance of more than 8 \AA .

Thus, allosteric inhibition of the protein takes place when treated with GTPs as observed earlier with RNase A.^[14] Interestingly, unlike the free ECG and EGCG, the polyphenol-capped AuNPs show competitive binding with very low K_i values ($\sim 4 \mu\text{g/ml}$). AuNPs act as nanocarriers and show efficient transport of the polyphenol to the target site, thereby increasing the local concentration of the polyphenol. It can be observed that the K_i value decreases by, $\sim 77\%$ for ECG and $\sim 73\%$ for EGCG in case of nanoparticles (Table 3). The results indicate that the spherical nanoparticles can show better binding with the active site of the protein and the Lineweaver-Burk plots suggest that the mode of inhibition is competitive which means that the inhibitor

binds to the active site. Upon binding, the spherical NP reduces the exposure of the active site residues of the protein towards the substrate thereby reducing the catalytic efficiency and increasing the efficiency of inhibition.

In order to further quantify the extent of nanoparticle binding with Ang, fluorescence quenching studies have been performed. A decrease in fluorescence intensity was observed on successive addition of the ligand to Ang in 20 mM phosphate buffer (pH 7.4; Figure 8). As shown in the docking studies, the polyphenol compounds are in very close proximity to the sole Trp residue, thereby decreasing its intrinsic fluorescence intensity. It is evident from the Stern-Volmer constant (K_{sv}) values that GTP-AuNPs show better inhibition than just the polyphenols and the linearity of the Stern-Volmer plot is in agreement with static quenching, and involves ground state complex formation with the fluorophore. The binding constant (K_b) and number of binding sites (n) of Ang with the ligands have been calculated at 25°C and are tabulated in Table 4, where GTPs show a single binding site. The K_b values obtained are in the order of 10^2 Lg^{-1} , with EGCG showing better binding among the polyphenols used. This can be attributed to the involvement of the phenolic-OH groups in the B and D rings which bind strongly with residues on

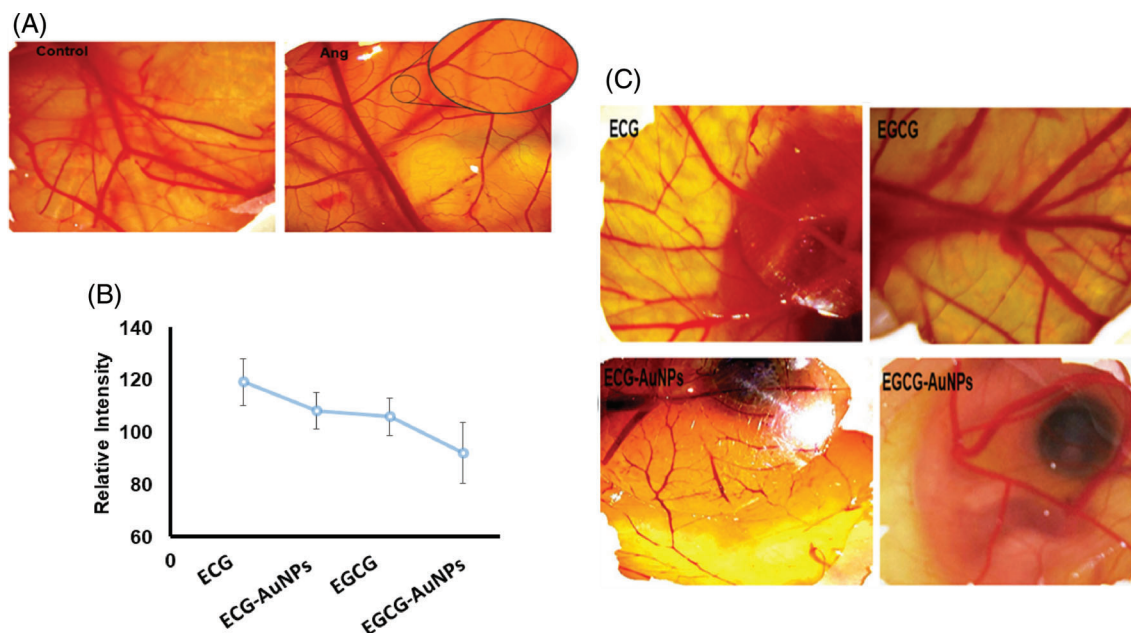


FIGURE 9 Effect of GTPs and GTP-AuNPs on angiogenesis in the CAM. A, Left: Control (Saline buffer, pH 7.4); Right: Ang (5 μ M/egg) in saline buffer. B, Angiogenesis was quantified by measuring the relative blood vessel intensity in absence and presence of various samples. Data are presented as Mean \pm SD with $P < 0.01$ compared to Ang group. C, The CAM assay of angiogenin induced angiogenesis process in presence of GTPs and GTP-AuNPs

the surface of the protein. Polyphenol-capped gold nanoparticles bind nearly 10^2 times more strongly to the protein compared to only the polyphenols.

Zeta potential values show that GTP-AuNPs are negatively charged at pH 7.4 and we know that Ang is positively charged at pH 7.4 as the pI is >9 . Therefore, it is expected that there would exist electrostatic interactions between GTP-AuNPs and Ang. The formation of AuNPs is stabilized by the reduction of Au (III) ($E^\circ \sim +0.99$ V)^[41] to Au (0) where GTPs act as the reducing agent as EGCG has an E° value of $\sim +0.42$ V and ECG $\sim +0.55$ V.^[42] The adjacent hydroxyl group of ring B of the GTPs forms a five membered ring that chelates the Au (III), and itself gets oxidized to quinones with concomitant reduction of Au(III) to Au(0). The AuNPs are thus stabilized by the phenolic compounds as well as quinones.^[43,44] This implies that the observed inhibition of Ang is likely to happen with ring D which protrudes outward and targets the hydrophilic amino acid residues of the protein, also observed from docking studies.

In fluorescence quenching experiments, the number of binding sites (n) describes the degree of cooperativity in protein-ligand binding, with the type of cooperativity determined by the value of the Hill coefficient.^[45] If ligand binding is enhanced by the presence of other ligands, then $n > 1$ and if the affinity for the binding of subsequent ligand molecules is decreased then the value of n is <1 . If $n = 1$, the binding of the ligand is independent of the binding of other ligands.

We observe that the value of n for EGCG-AuNPs is higher than 1, where, $n \approx 1.8$ and for ECG-AuNPs, $n \approx 1.0$ suggesting cooperative binding in case of EGCG-AuNPs. Whereas, the value of ' n ' for ECG-AuNPs indicates that the binding of the ligand is independent of the

binding of other ligands, but the extent of increase in the value of K_b compared to ECG can be a result of cooperative binding. This is in agreement with the binding constant value obtained from fluorescence quenching data which shows that the binding constant is relatively more for GTP-AuNPs compared to bare GTPs because of the binding of multilayer Ang on the surface of GTP-AuNPs and one binding stimulates the other ligand to bind, thus increasing the adsorption of protein. Higher binding in case of GTP-AuNPs can be a probable reason for the competitive nature of binding thus showing an enhancement in the inhibition efficiency of the nanoparticles. Cooperativity impacts both kinetic and thermodynamic properties of macromolecular ligand systems,^[46] where the formation of sigmoidal curve rather than a hyperbolic curve is obtained for a velocity versus [Substrate] plot in Michaelis-Menten kinetics. The occurrence of positive cooperative binding concluded by the formation of a sigmoidal kinetic profile for GTP-AuNPs compared to bare GTPs is provided in Figure S2.

An *in vivo* study was performed to observe the effect of the purified protein and the small molecules which were analyzed as inhibitors of angiogenin by previously mentioned *in vitro* assays. CAM assay shows the angiogenic activity of the purified Ang, as observed by the proliferation of the blood vessels compared to the control set (the inset of the image shows an increase in the branching of the blood vessel (Figure 9A).

The inhibitor efficacy of the samples was assessed by measuring the number of blood vessels formed, using Kodak MI software. A comparative histogram of relative blood vessels formed for various polyphenols has been plotted in Figure 9B, where the polyphenols and polyphenol-capped gold nanoparticles were found to suppress blood vessel growth in comparison to Ang.

Among the inhibitors used, EGCG-AuNPs are the most effective against angiogenin induced angiogenesis (Figure 9C), which agrees with the results of the *in vitro* assays. The lower intensity of the blood vessels for the samples preincubated with angiogenin indicates their anti-angiogenic activity, which focuses on their potential to behave as pharmaceutical targets for anti-angiogenesis. Among the samples used, polyphenol-capped gold nanoparticles (GTP-AuNPs) show better anti-angiogenic potency compared to the bare polyphenols (GTPs).

4 | CONCLUSION

The results and data presented in this study support our speculation on the importance of gallate containing moieties in green tea polyphenols. Increase in the binding constant values and decrease in the inhibition constant values provide us with sufficient information about their increased efficiency as inhibitors of the ribonucleolytic activity of Ang. Results on RNase A inhibition with metal chelates of green tea polyphenols have also been reported.^[47] The idea of using nanocarriers to increase the bioavailability of the polyphenols have provided a way to increase the efficacy of the inhibition of the ribonucleolytic activity of the protein. Spectroscopic methods help us to investigate the competitive and cooperative binding of the formed negatively charged EGCG-AuNPs in the inhibition of Ang. The *in vivo* studies of the protein show that the angiogenin induced angiogenesis process can be inhibited by the polyphenols which not only act as inhibitors against the ribonucleolytic activity of angiogenin but also exhibit anti-angiogenic properties. The use of GTP-AuNPs in the CAM assay (day 10), where almost no branching of the blood vessel occurs elicits its ability to act as an efficient anti-angiogenic agent. With the exact knowledge of the ligand binding site and the specific mode of inhibition depending on the residues involved, further study of the rational design of such compounds has potential.

ACKNOWLEDGMENTS

Swagata Dasgupta acknowledges Council of Scientific and Industrial Research, India (CSIR, Project No.: 01(2959)/18/EMR-II) for financial support. Authors are grateful to IIT Kharagpur and CRF for financial support and instrument facilities. The authors would like to thank Prof. Amit Kumar Das for providing us the bacterial strains and Prof. D. Dhara and his laboratory (Department of Chemistry, IIT Kharagpur) for assisting with DLS experiments.

CONFLICT OF INTEREST

The authors declare no conflict of interest.

DATA AVAILABILITY STATEMENT

The data that support the findings of this study are available from the corresponding author upon request.

ORCID

Swagata Dasgupta  <https://orcid.org/0000-0003-2074-1247>

REFERENCES

- [1] T. Tsuji, Y. Sun, K. Kishimoto, K. A. Olson, S. Liu, S. Hirukawa, G. F. Hu, *Cancer Res.* **2005**, *65*, 1352.
- [2] R. Shapiro, J. F. Riordan, B. L. Vallee, *Biochemistry* **1986**, *25*, 3527.
- [3] D. J. Strydom, J. W. Fett, R. R. Lobb, E. M. Alderman, J. L. Bethune, J. F. Riordan, B. L. Vallee, *Biochemistry* **1985**, *24*, 5486.
- [4] S. Weremowicz, E. A. Fox, C. C. Morton, B. L. Vallee, *J. Hum. Genet.* **1990**, *47*, 973.
- [5] R. Shapiro, *Biochemistry* **1998**, *37*, 6847.
- [6] J. W. Harper, B. L. Vallee, *Biochemistry* **1989**, *28*, 1875.
- [7] A. P. Leland, K. E. Staniszewski, et al., *Biochemistry* **2002**, *41*, 1343.
- [8] a) A. Russo, K. R. Acharya, R. Shapiro, *Methods Enzymol.* **2001**, *341*, 629. b) N. Russo, K. R. Acharya, B. L. Vallee, R. Shapiro, *Proc. Natl. Acad. Sci. U. S. A.* **1996**, *93*, 804. c) R. Y. Kao, J. L. Jenkins, K. A. Olson, M. E. Key, J. W. Fett, R. Shapiro, *Proc. Natl. Acad. Sci. U. S. A.* **2002**, *99*, 10066.
- [9] Y. Cao, R. Cao, *Nature* **1999**, *398*, 381.
- [10] K. S. Ghosh, T. K. Maiti, S. Dasgupta, *Biochem. Biophys. Res. Commun.* **2003**, *308*, 64.
- [11] K. S. Ghosh, T. K. Maiti, S. Dasgupta, *Biochem Biophys Res Commun* **2004**, *325*, 807.
- [12] S. M. Chacko, P. T. Thambi, R. Kuttan, I. Nishigaki, *Chin Med* **2010**, *5*, 13.
- [13] Y. D. Jung, L. M. ELLIS, *Int J Exp Pathol.* **2001**, *82*, 309.
- [14] K. S. Ghosh, T. K. Maiti, J. Debnath, S. Dasgupta, *Proteins* **2007**, *69*, 566.
- [15] S. M. Rybak, B. L. Vallee, *Biochemistry* **1988**, *27*, 2288.
- [16] N. Russo, R. Shapiro, K. R. Acharya, J. F. Riordan, B. L. Vallee, *Proc. Natl. Acad. Sci. U. S. A.* **1994**, *91*, 2920.
- [17] R. Shapiro, B. L. Vallee, *Biochemistry* **1989**, *28*, 7401.
- [18] D. G. Anderson, G. G. Hammes, F. G. Walz, *Biochemistry* **1968**, *7*, 1637.
- [19] L. H. Bowman, B. Rabin, D. Schlessinger, *Nucleic Acids Res.* **1981**, *9*, 4951.
- [20] D. D. Leonidas, R. Shapiro, S. C. Allen, G. V. Subbarao, K. Veluraja, K. R. Acharya, *J. Mol. Biol.* **1999**, *285*, 1209.
- [21] H. M. Berman, J. Westbrook, Z. Feng, G. Gilliland, T. N. Bhat, H. Weissig, I. N. Shindyalov, P. E. Bourne, *Nucleic Acids Res.* **2000**, *28*, 235.
- [22] W. L. DeLano, *The PyMOL Molecular Graphics System*, DeLano Scientific, SanCarlos, CA, USA **2002**. <http://www.pymol.org>.
- [23] O. Trott, A. Olson, *J. Comput. Chem.* **2010**, *31*, 455.
- [24] Hubbard SJ, Thornton JM. "NACCESS" Computer Program, Department of Biochemistry and Molecular Biology, University College, London, **1993**.
- [25] B. D. Smith, M. B. Soellner, R. T. Raines, *J. Biol. Chem.* **2003**, *278*, 20934.
- [26] R. G. Tantiado, V. P. Tan, *Int. J. Bio-Sci. Bio-Tech.* **2012**, *4*, 93.
- [27] E. W. Miles, *Methods Enzymol.* **1977**, *47*, 431.
- [28] J. Y. Chung, C. Huang, X. Meng, Z. Dong, C. S. Yang, *Cancer Res.* **1999**, *59*, 4610.
- [29] W. J. Lee, J. Y. Shim, B. T. Zhu, *Mol. Pharmacol.* **2005**, *68*, 1018.
- [30] R. Shapiro, J. W. Harper, E. A. Fox, H. W. Jansen, F. Hein, E. Uhlmann, *Anal. Biochem.* **1988a**, *175*, 450.
- [31] N. Russo, K. R. Acharya, B. L. Vallee, R. Shapiro, *Proc. Natl. Acad. Sci. U. S. A.* **1996**, *93*, 804.
- [32] J. Moroianu, J. F. Riordan, *Proc. Natl. Acad. Sci. U. S. A.* **1994a**, *91*, 1677.
- [33] J. Moroianu, J. F. Riordan, *Biochem. Biophys. Res. Commun.* **1994b**, *203*, 1765.
- [34] M. V. Nogue's, M. Vilanova, C. M. Cuchillo, *Biochim. Biophys. Acta* **1995**, *1253*, 16.
- [35] A. R. Shafiq, A. Abdul Aziz, B. Mehrdel, *J. Phys. Conf. Ser.* **2018**, *1083*, 012040.

- [36] N. M. O'Boyle, M. Banck, C. A. James, C. Morley, T. Vandermeersch, G. R. Hutchison, *Aust. J. Chem.* **2011**, 3, 33.
- [37] I. Rajendran, H. Dhandapani, R. Anantanarayanan, R. Rajaram, *RSC Adv.* **2015**, 5, 51055.
- [38] S. Chavva, S. Deshmukh, R. Kanchanapally, N. Tyagi, J. Coym, A. Singh, S. Singh, *Nanomaterials* **2019**, 9, 396.
- [39] D. S. Hsieh, H. C. Lu, C. C. Chen, C. J. Wu, M. K. Yeh, *Int. J. Nanomed.* **2012**, 7, 1623.
- [40] B. Yuval, *Chem. Biol. Drug Des.* **2010**, 75, 535.
- [41] K.V. Katti, R. Kannan, Stabilized, biocompatible gold nanoparticles and enviro-friendly method for making same, USA 8,333,994, **2016**
- [42] F. Balz, J. V. Higdon, *J Nutr* **2003**, 133, 3275S.
- [43] X. Huang, H. Wu, X. Liao, B. Shia, *Green Chem.* **2010**, 12, 395.
- [44] R. Majumdar, B. G. Bag, *Int.J: Res. Chem. Environ* **2012**, 2, 338.
- [45] J. N. Weiss, *FASEB J.* **1997**, 11, 835.
- [46] C. M. Porter, B. G. Miller, *Bioorg. Chem.* **2012**, 43, 44.
- [47] K. S. Ghosh, T. K. Maiti, A. Mandal, S. Dasgupta, *FEBS Lett.* **2006**, 580, 4703.

SUPPORTING INFORMATION

Additional supporting information may be found online in the Supporting Information section at the end of this article.

How to cite this article: Panda A, Karhadkar S, Acharya B, Banerjee A, De S, Dasgupta S, *Biopolymers* **2021**, 112, e23429.
<https://doi.org/10.1002/bip.23429>